



Design and Test of the MEMS Coupled Piezoelectric–Electromagnetic Energy Harvester

Lian-min Cao¹ · Zhi-xu Li¹ · Cheng Guo¹ · Peng-peng Li¹ · Xiang-qiang Meng¹ · Ting-ming Wang¹

Received: 4 July 2018 / Revised: 2 October 2018 / Accepted: 21 October 2018 / Published online: 11 February 2019
© Korean Society for Precision Engineering 2019

Abstract

This paper researches on the design and test of the output performance of double-end clamped MEMS coupled piezoelectric–electromagnetic energy harvester. It establishes the theoretical output model of the double-end clamped rectangular beam and trapezoidal beam piezoelectric–electromagnetic energy harvester, and optimizes the structure parameters of piezoelectric and electromagnetic unit with simulation analysis. It also respectively realizes the processing of piezoelectric and electromagnetic unit by MEMS and flexible PCB technology, and completes the performance test of structure prototype through the experimental system. The result showed that the capacity of MEMS coupled piezoelectric–electromagnetic energy harvester, which taked four coil piezoelectric with integrated electromagnetic in series, was 12.23 times higher than that of piezoelectric energy harvester. Also the output voltage and power of coupled trapezoidal beam energy harvester were respectively increased 18.89% and 2.26%, compared with coupled rectangular beam energy harvester.

Keywords Coupled energy harvester · Piezoelectric · Electromagnetic · MEMS · Double-end clamped

List of Symbols

t	Time
m_e	Equivalent mass
c_e	Equivalent damping
k	Equivalent stiffness
k_1, k_3	Nonlinear stiffness introduced by large deformation
θ	Coupling coefficient of piezoelectricity
γ	Coupling coefficient of electromagnetism
$z(t)$	Displacement function
$V(t)$	Piezoelectric partial voltage function
$i(t)$	Electromagnetic partial current function
$a(t)$	Acceleration
μ	Calibration factor of the energy harvester system model
R_1	Loading resistance of the piezoelectric part
R_2	Internal equivalent resistance
R_3	Loading resistance of the electromagnetic part
C	Equivalent capacitance of the piezoelectric part
L	Equivalent inductance of the electromagnetic part

1 Introduction

In recent years, with the continuous development of wireless sensor network, field intelligent sensing system, environmental monitoring system, personal wearable system and other fields, the energy supply problem of these smart sensor systems has become the key to restrict its development [1–3]. With the development of vibrational energy harvest technology, it is possible to convert the vibration energy in the environment into electrical energy for the energy supply of the sensor.

A great number of research work has been done on the piezoelectric energy harvester and the electromagnetic energy harvester. It concludes that the piezoelectric energy harvester has larger output voltage, but smaller output current from a few to tens of microamperes, due to the large resistance, which is suitable for working in high loading environment; in addition electromagnetic energy harvester has larger output current, but smaller output voltage from tens to hundreds of millivolts, which is unable to meet the general requirements of rated voltage devices, and suitable for working in smaller loading environment [4]. Therefore, considering the output characteristics and performance complementarity of these two energy harvesters, the researchers put forward the combination of two energy harvest mechanisms of piezoelectric and electromagnetic in the same

✉ Lian-min Cao
skdclm@163.com

¹ College of Mechanical and Electronic Engineering, Shandong University of Science and Technology, Qingdao 266590, China

structure, which can output large voltage and large current simultaneously. At present, the coupled piezoelectric–electromagnetic energy harvester has become a hot spot and trend of vibration energy harvest.

Wacharasindhu designed the keyboard power of coupled piezoelectric–electromagnetic energy harvester, and PZT thin films and planar coil, based on d33 mode, are achieved by the MEMS processing [5]. When tapping the keyboard on the magnet under vibration, changes occur, the magnetic flux through the coil is also due to the magnet stress effect on PZT. Then the coil and the PZT layer will output power. According to experiment, the output power of piezoelectric and electromagnetic energy harvest unit is respectively 40.8 μW and 1.15 μW . Yang designed two kinds of coupled piezoelectric–electromagnetic energy harvester according to the location of magnet and coil, and the structure was processed by micro-machining process [6]. Under the excitation of 2.5 g, the output power of the piezoelectric and electromagnetic energy harvest units are 107 μW and 0.18 μW respectively, when the coil is directly under the magnet. When the coil is on the side of the beam, and the direction of the magnetic pole is perpendicular to the plane of the coil, the output power of the piezoelectric and electromagnetic energy harvest units are 176 μW and 0.19 μW respectively. Challa designed a small coupled piezoelectric and electromagnetic energy harvester, which adheres to the piezoelectric plate on the surface of the cantilever beam, and the magnet is fixed to the end of the beam, and a winding circle is placed in the bottom of the magnet [7]. Through the theoretical analysis of the matching relation between the mechanical damping and electrical damping, the coupled piezoelectric–electromagnetic energy harvester can increase the output power of energy harvesting structure, compared to a piezoelectric or electromagnetic energy harvester with a single energy harvest mechanism. According to the test results, the first-order resonant frequency of the structure is 21.6 Hz, while the output power of the piezoelectric energy harvester and electromagnetic energy harvester are 257 μW and 244 μW respectively, while the output power of the coupled is 332 μW . Robert et al. [8] also shows that the output power of the coupled energy harvester is better than that of the piezoelectric energy harvester and the electromagnetic energy harvester, and the coil in the electromagnetic energy harvest unit can also be applied to the inductance in the SSHI circuit to increase the output power of the high voltage electric energy harvest unit. Tadesse et al. [9] designed a multimodal coupled piezoelectric–electromagnetic energy harvester based on a cantilever beam mass block. The study shows that the electromagnetic energy harvest unit can output larger power in the low frequency vibration environment, while the piezoelectric harvest unit has greater output power at high frequency vibration. Therefore, the combination of the two energy harvesting mechanisms

can broaden the range of the energy harvesting band. Zhang Yating and Chen Tingting designed four clamped beam mass structure of coupled micro piezoelectric–electromagnetic energy harvester based on composite type, the experimental test, in the acceleration excitation of 6 g, the peak output voltage of the piezoelectric unit is 94 mV, although the peak output voltage of electromagnetic unit is 8 mV, the output signal is quite unstable. Li has studied the electromechanical coupling characteristics, the random output response and the output characteristics of the piezoelectric–electromagnetic energy harvester under the nonlinear action. The research has shown that to increase the electromechanical coupling and nonlinear force can also increase the output power and the energy harvest bandwidth of the energy harvester [10–13].

Through the above investigation and analysis, the best design criteria of the coupled energy harvester in the literature are rarely mentioned. A lot more work should be done to design the coupled piezoelectric–electromagnetic energy harvest structure with excellent performance. Considering the vibration frequency in the work environment is usually distributed in a certain frequency range, if the harvester has narrow bandwidth, it can only work in the smaller frequency range, and reduce the energy harvesting efficiency. Therefore, we need to broaden the transducer bandwidth, in order to cover the vibration frequency in the entire working environment, improve the energy harvesting efficiency, and increase the output power.

The paper has designed the MEMS coupled piezoelectric–electromagnetic energy harvester. The structure of piezoelectric part has double-end clamped rectangular four beam structure and double-end clamped trapezoidal beam, in which double-end clamped rectangular four beam structure is used to increase the series output voltage, and double-end clamped trapezoidal beam is used to optimize the output power. The electromagnetic part consists of a micro planar coil and a micro high performance permanent magnet. In the study, we optimize and make the MEMS micro processing the structure of energy harvest, and finally tests the output performance of the micro coupled piezoelectric–electromagnetic energy harvester prototype.

2 Theoretical Model of MEMS Double-End Clamped Beam Structure

For the double-end clamped beam structure, when the structure has small displacement (small deformation), the neutral surface is not elongated. There is a positive and negative strain distribution on both sides of the neutral surface [14]. On the same surface, the direction of strain on the two sides of the center of the beam is opposite, as shown in Fig. 1a. When the beam has large displacement (large deformation),

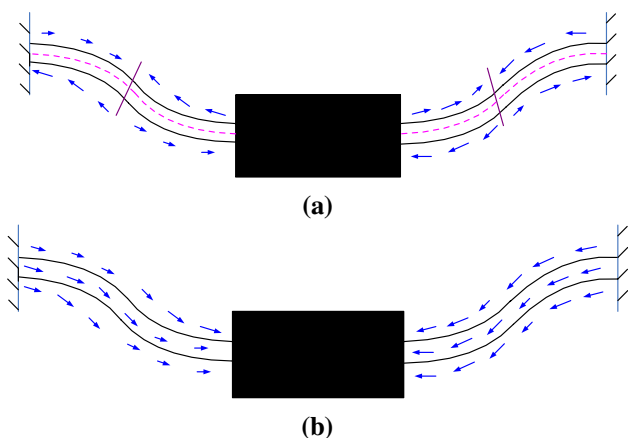
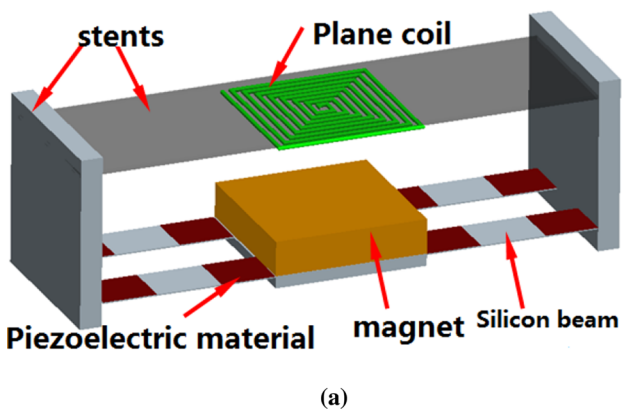


Fig. 1 Bending stress and tensile stress distribution: **a** bending stress in small deformation; **b** tensile stress in large deformation

the neutral surface of the beam will be stretched, and the tensile stress take effect on the beam in the same direction, such as Fig. 1b [15, 16].

After introducing the nonlinear factors of large deformation, the state equation of the coupled piezoelectric–electromagnetic energy harvester can be expressed as:

$$\begin{cases} m_e \frac{d^2 z(t)}{dt^2} + c_e \frac{dz(t)}{dt} + kz(t) + k_1 z(t) + k_3 z^3(t) + \theta V(t) + \gamma i(t) = \mu m_e a(t) \\ \frac{V(t)}{R_1} + C \frac{dV(t)}{dt} - \theta \frac{dz(t)}{dt} = 0 \\ L \frac{di(t)}{dt} + (R_2 + R_3)i(t) - \beta \frac{dz(t)}{dt} = 0 \end{cases} \quad (1)$$



3 Design of MEMS Double-End Clamped Beam Structure

3.1 Design of Rectangular Beam Structure Energy Harvester

Due to the limitation of processing technology, the thickness of detection quality (silicon material) can only reach to 220 μm at most in the optimal design, and the thickness of PZT piezoelectric material can only reach to 1.3 μm at most. Therefore, Fig. 2 shows the designed original size of the prototype structure (4000 μm long beam, beam breadth 1725 μm, symmetrical stick two pieces of PZT, on a beam with beam breadth, width of PZT PZT length 1950 μm). On this basis, we have optimized the design of the breadth and length of the beam, and width of PZT, researched on the structure of the output voltage and equivalent power, so as to get the best shape of structure.

By means of simulation software ANSYS, we get the first resonance frequency with the modal analysis, and through the harmonic response analysis, obtain corresponding voltage data structure. On this basis, output power is calculated according to the structure parameters. This part will optimize the design by changing the beam width, beam length and PZT material length, so as to get the optimal structure. In addition, a comparative analysis is made on the rectangular beam and trapezoidal beam of MEMS double-end clamped beam.

By using ANSYS software, the optimal beam length, beam width and PZT width are selected and the simulation was carried out under the conditions of other parameters unchanged.

Through the comparison and analysis of the simulation, it results that the optimized structure has a great increase in voltage and power, which the voltage is increased 99.43%

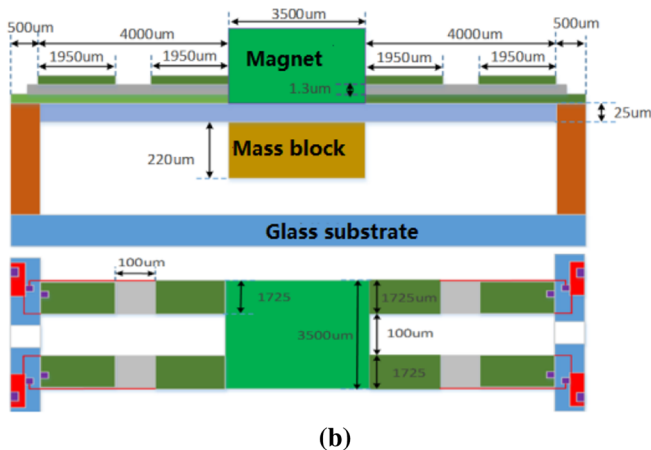


Fig. 2 Coupled piezoelectric–electromagnetic energy harvester prototype and MEMS structure size parameter

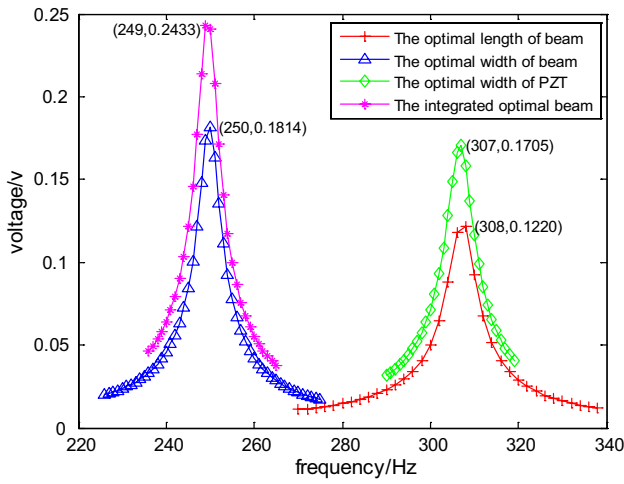


Fig. 3 Frequency–voltage contrast diagram

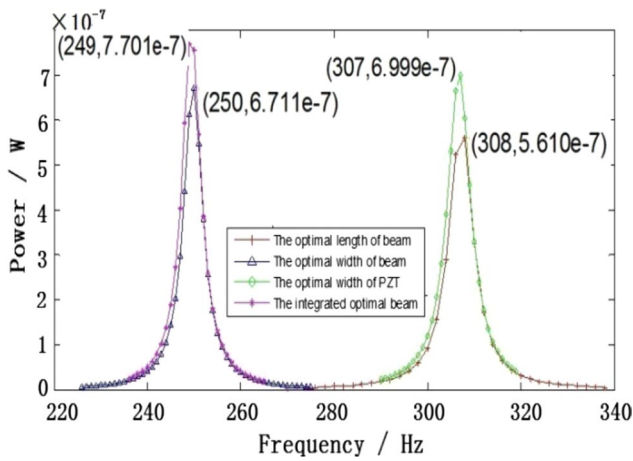


Fig. 4 Frequency–power contrast diagram

and the power is increased 37.27%. The four sets of structures bandwidth are between 5 and 6.5 Hz with inapparent difference (Figs. 3, 4, 5).

3.2 Comparison and Analysis of MEMS Double-End Clamped Rectangular Beam and Trapezoid Beam

In order to improve the output performance of the piezoelectric structure, the ANSYS software is used to simulate the double-end clamped rectangular beam and trapezoid beam. The structure model and the grid are shown in Figs. 6 and 7. The first order modal displacements, stress and strain structure of a double- end clamped rectangular beam and trapezoid beam are compared and analyzed.

From the comparison result, the trapezoid beam has greater displacement and more uniform distribution of stress and strain than the rectangular beam structure. The center

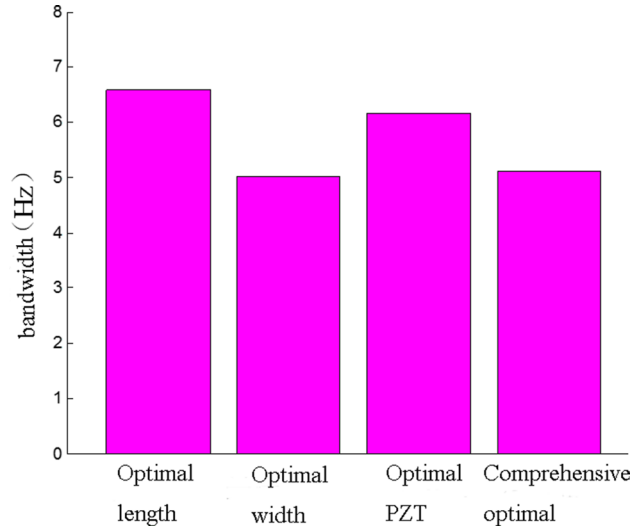


Fig. 5 Bandwidth contrast diagram

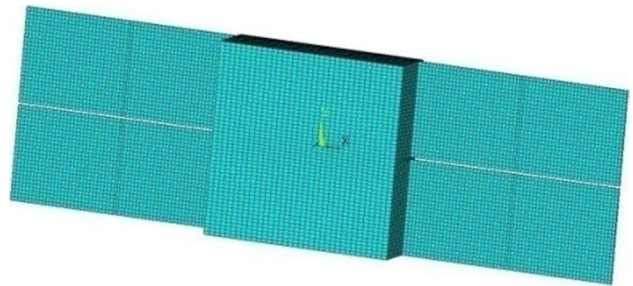


Fig. 6 Structure model of rectangular beam

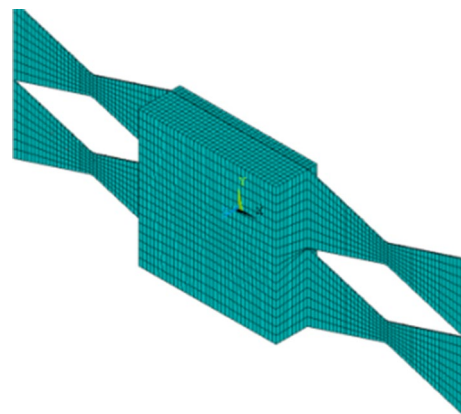


Fig. 7 Structure model of trapezoid beam

line (x direction) of the bottom surface of a beam is used as the research object to observe the strain distribution.

From the graph, we can see that the larger stress and strain are mainly concentrated on the constraint ends of the beam and the connection between the beam and the

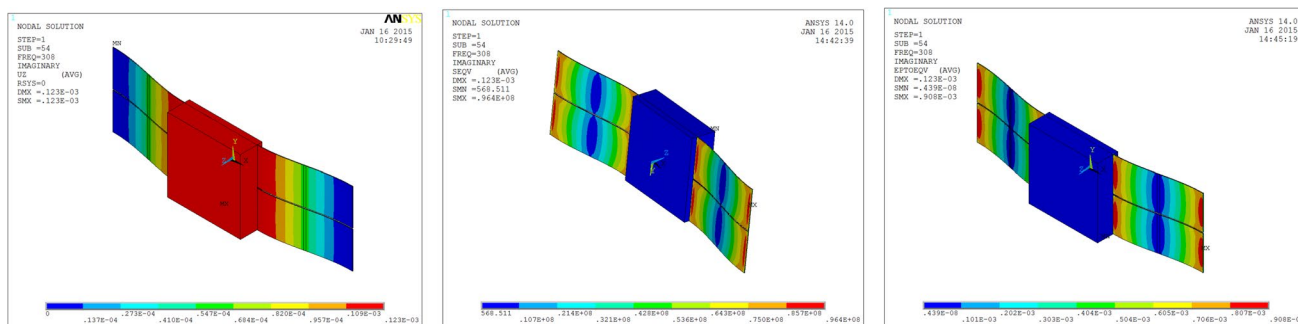


Fig. 8 The first order model displacement and first order stress and first order strain of rectangular beam

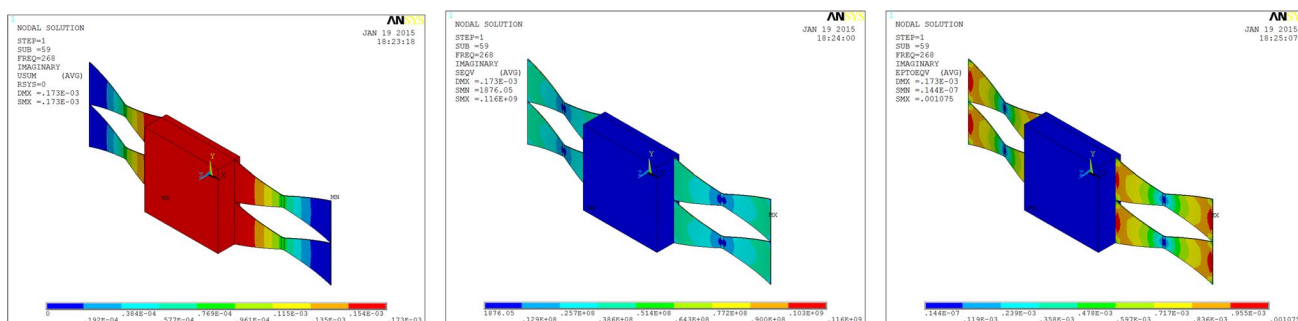


Fig. 9 The first order model displacement and first order stress and first order strain of trapezoid beam

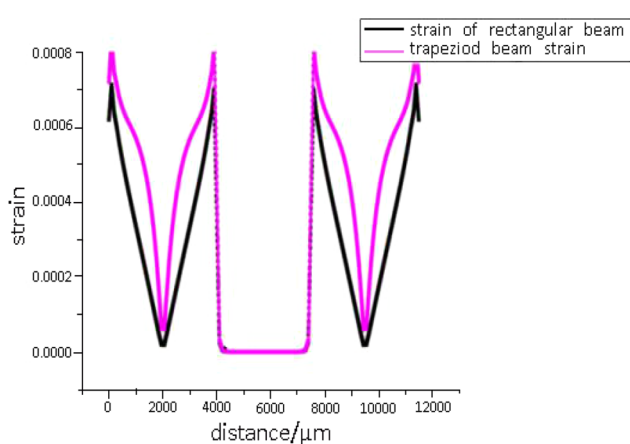


Fig. 10 Strain graph along the middle line

mass block. The middle part of the beam bears less stress and strain, and the thinning of the beam has little effect on the strength of the beam. While changing to the trapezoidal beam, the displacement increased 40.07%, the

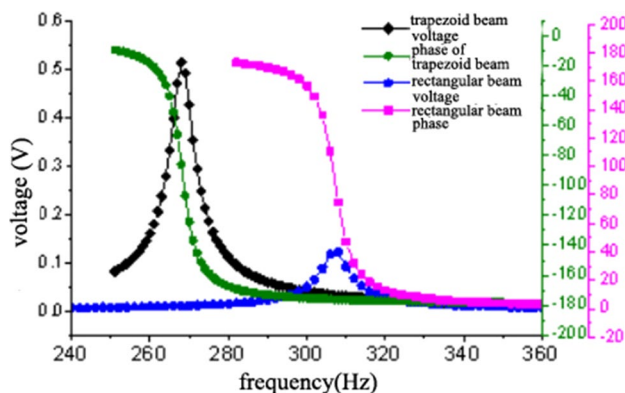


Fig. 11 Voltage comparison diagram

stress increased 22.69%, and the strain increased 17.01% (Figs. 8, 9, 10, 11, 12).

The analysis shows that the output voltage of the trapezoid beam is 5 times than that of the rectangular beam in the same size, and the power is about 10 times than that of the rectangular beam in the same size.

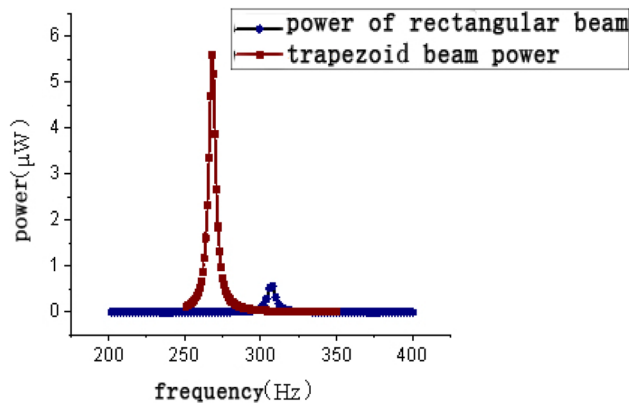


Fig. 12 Power comparison diagram

4 Processing of the Piezoelectric Energy Harvester with Double-End Clamped Beam

For the optimized structure, MEMS processing mainly involves two major processes: bulk silicon micro-processing and PZT film preparation processing, in which, bulk silicon processing includes silicon processing and non-silicon (silicon oxide and silicon nitride silicon etc.) processing, lithography and electrode magnetron sputtering; PZT film preparation processing includes PZT suspension preparation, and the key techniques of film firing and film graphic. MEMS piezoelectric structure and the processing flow are shown in Figs. 13 and 14. After depositing SiO_2 on in the silicon, the beam is fabricated by the etching process. Then, PZT thin film is prepared by sol-gel method on the beam, where Ti and Pt are used as the top and down electrode. In the fabrication, it needs to ensure the integrity of PZT layer and avoid the interconnection of top electrode and bottom electrode. Besides, it needs to check there are no cracks on the surface of PZT layer. These aspects always result in the failure or lower power output for MEMS piezoelectric energy harvester. The structure after processing is shown in Fig. 15.

The electromagnetic unit coil is realized by flexible PCB process, with the thickness of 1 mm and 6 layers of the coil. The structure after processing is shown as below (Fig. 16).

5 Performance Test of MEMS Coupled Piezoelectric and Electromagnetic Energy Harvester

A corresponding test system was designed, as shown in Fig. 17. Sinusoidal excitation signal generated from signal generator, is connected with the vibration table through the power amplifier; MEMS piezoelectric structure and

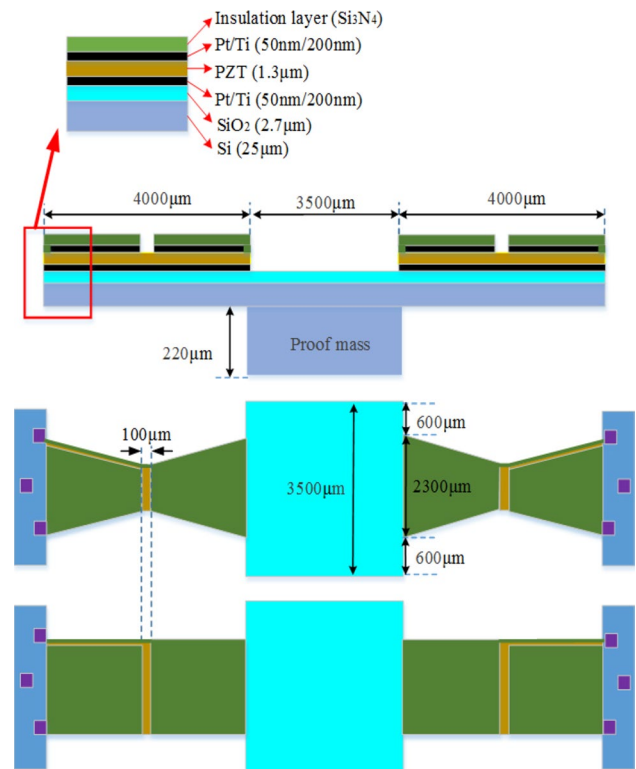


Fig. 13 MEMS piezoelectric structure

accelerometer are fixed on the vibration platform; the output data of piezoelectric structure is displayed through the oscilloscope; accelerometer signal is displayed through the signal analyzer; the amplitude of the MEMS piezoelectric structures is achieved by high-speed camera, and recorded by the computer; the news lamp is used to lighten high speed camera. The piezoelectric part of the coupled piezoelectric–electromagnetic energy harvester is four-beam structure, in order to improve the output voltage; the electromagnetic part is the permanent magnet quality detection of planar coils and permanent magnets, which the size is 3.5 mm * 3.5 mm * 0.8 mm, and the performance is N52; the coil is the planar flexible coil, equal to the quality detection area, and single coil resistance is 5.2 Ω . The magnitude of the acceleration is set up to 2 m/s^2 in order to facilitate the comparison and analysis of the piezoelectric structure test.

5.1 Four Beam Structure with Double-End Clamped Beam and Piezoelectricity Test

5.1.1 Vibration Response Test

A high-speed camera is used to analyze the mechanical vibration response of MEMS structure. The test points are set up on the side of beam quality detection, and the vibration amplitude of test points is detected as the amplitude

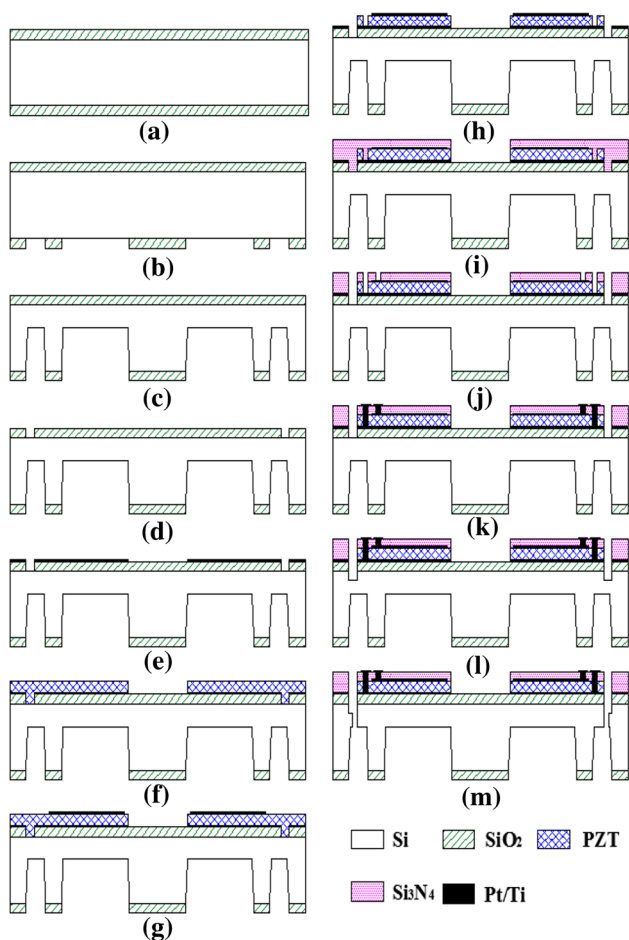


Fig. 14 Processing flow

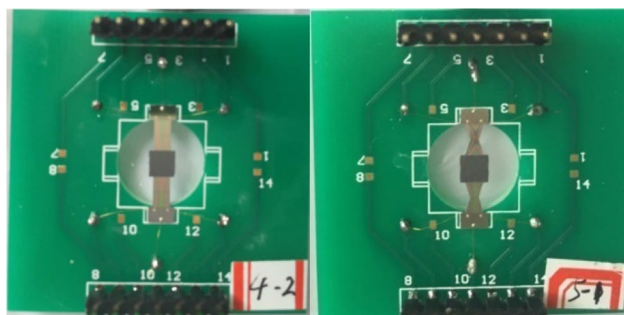


Fig. 15 The structure of MEMS piezoelectric rectangular beam and trapezoid beam after processing

data of beam vibration. The test charts and data are shown in Figs. 18, 19 and 20. The test structure shows that the resonant amplitude can reach to 208 μm , and the damping ratio of the MEMS four beam structure is 0.0157 when working in the air.

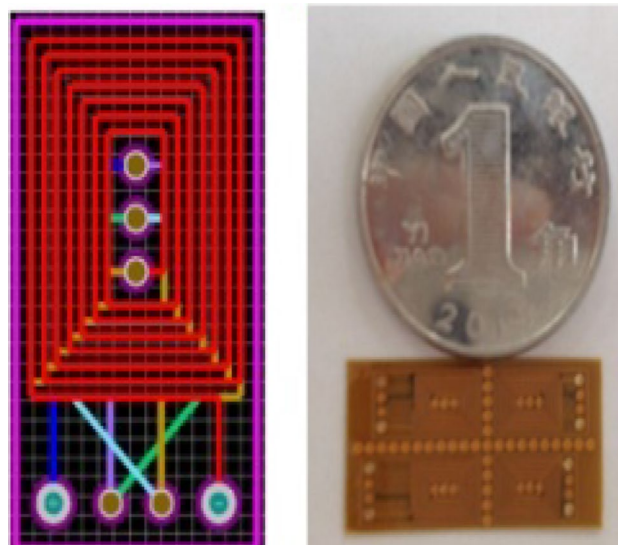


Fig. 16 Beam structure after processing

5.1.2 Piezoelectric Performance Test

In view of the MEMS piezoelectric energy harvesting characteristics, the piezoelectric energy harvesting test is carried out and the results are shown in Figs. 21 and 22. In the two piezoelectric layers laid on a single piezoelectric beam, the peak value of each opening circuit voltage is 34.6 mV, and the output voltage of the piezoelectric layer near the detection quality is slightly smaller than that of the piezoelectric layer near the constraint end. A single beam and two piezoelectric layers are connected in series, and the peak value of the output opening circuit is 50.1 mV. The opening voltage of the four beam in series is up to 0.24 V.

The optimum loading of single block piezoelectric layer is 20 K Ω , and the maximum output power is 7.61 nW; the series power of two pieces of piezoelectric layer of single beam is 8.61 nW. It can be seen that due to the nonlinear axial force of the beam, the mode of the original small deformation is changed, and the strain of the piezoelectric layer near the detection mass is weakened, while the strain near the constraint part is enhanced, so that the output voltage of the former is lower than that of the latter (Tables 1, 2).

5.2 Test of Coupled Piezoelectric–Electromagnetic Energy Harvester with Rectangular Beams

In order to make full use of space and improve the power density, the piezoelectric energy harvester is improved to coupled piezoelectric–electromagnetic energy harvester, namely, there sets up a planar coil above the quality detection (permanent magnet), and designs a distance adjusting device between the coil and the permanent magnet with the usage of the magnetic material, as shown in Fig. 23.

Fig. 17 MEMS piezoelectric energy harvester test system

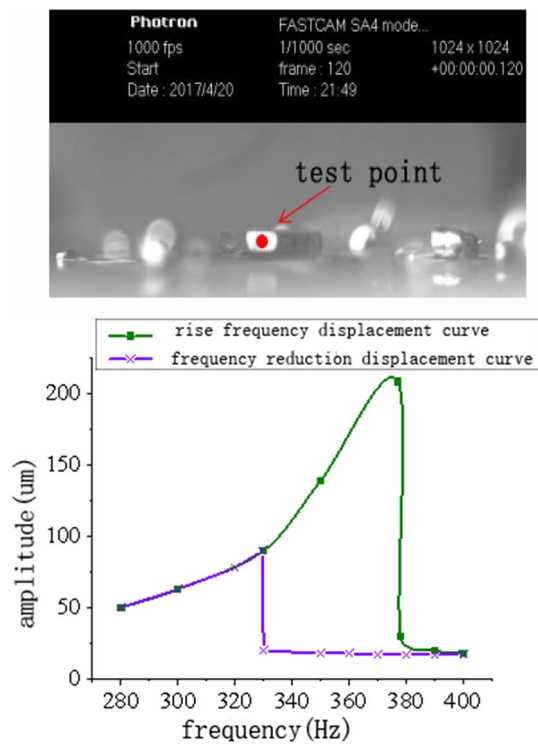
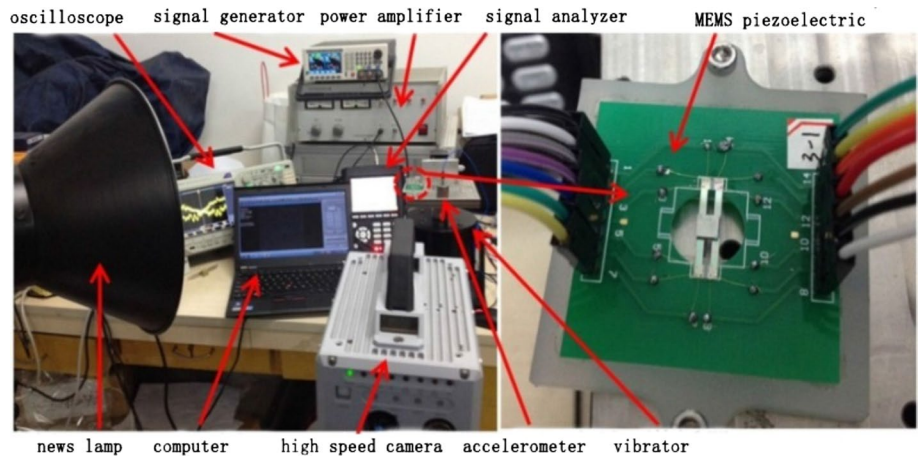


Fig. 18 Amplitude test and result

We make use of the coupled energy harvester structure to measure the electromagnetic output performance separately. The number of coil layers is changed in the test. The distance between the coil and the permanent magnet in the test is fixed to 1 mm. The test results are shown in Figs. 24 and 25. The output opening circuit voltage, the capture bandwidth and the optimal loading power are

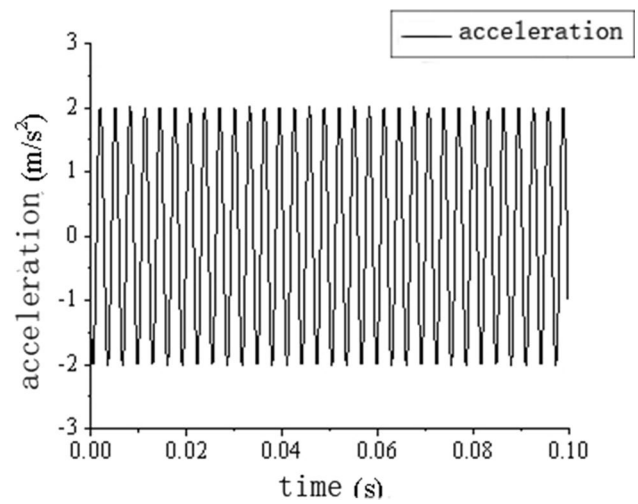


Fig. 19 Acceleration test

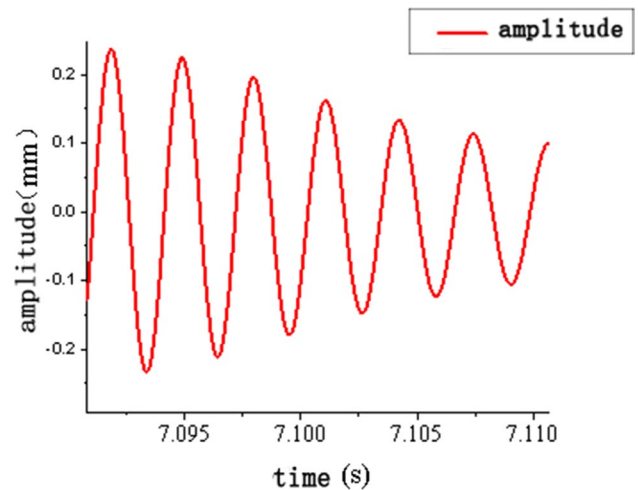


Fig. 20 Damping ratio test

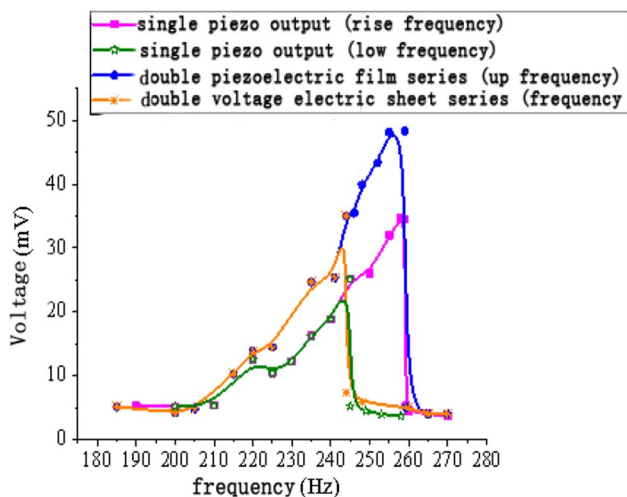


Fig. 21 Opening circuit voltage of single beam

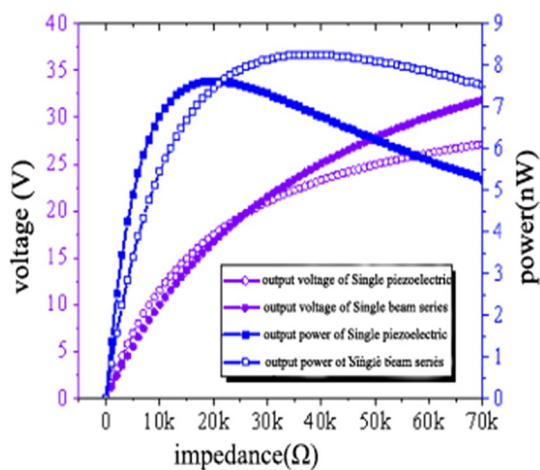


Fig. 22 Loading characteristics of single beam

Table 1 Optimal structure data table

Parameter	Beam width	Beam length	PZT length
Numerical (μm)	1150	4000	1250

increasing with the increase of the number of coil layers. The more coil layers increase, the more obvious the nonlinearity is, the higher the frequency of the maximum

opening circuit voltage. The peak values of opening circuit voltage of single layer, two layer and four layer coils are 2.05 mV, 4.65 mV and 8.60 mV respectively. The output power results (Fig. 25) show that the optimal loading increases in turn with the increase of the number of coil layers, and the output power is 0.101 mW, 0.270 mW and 0.462 mW in turn.

In order to improve the output performance of the coupled energy harvester, four kinds of coupled energy harvester are designed based on single piezoelectric and single electromagnetic tests. The parameters setting is shown in Table 3.

The results of the test are shown in Figs. 26 and 27 and Table 4. Through comparative analysis, the following results can be obtained: (1) The output performance can be improved by the series of piezoelectric wafers and increasing the coil. (2) The performance of electromagnetic output is outstanding, and it has little influence on the piezoelectric output. (3) The output power of the single MEMS piezoelectric energy harvesting can be increased for 12.23 times by using the electromagnetic four coil and the piezoelectric series. (4) The energy harvesting bandwidth of the coupled energy harvester is significantly improved than that of the single piezoelectric energy harvester, and the energy harvesting frequency band is widened nearly 4 times.

5.3 Output Performance of Coupled Piezoelectric–Electromagnetic Energy Harvester with Trapezoid Beam

We change the piezoelectric structure of the original rectangle to a trapezoid piezoelectric structure with more uniform strain on the surface of the beam, and design a comparative analysis test. In order to further analyze the energy harvesting characteristics of trapezoidal beam and rectangular beam structure, the 5th coupled energy harvester and the 6th coupled energy harvester are designed, and the related structural parameters are shown in Table 5.

The output performance of the 5th and the 6th coupled energy harvesters are shown in Figs. 28, 29 and 30 and Table 6. Through comparative analysis, the following results can be obtained: the resonant frequency of 6th coupled energy harvester (trapezoidal beam) is lower than the 5th coupled energy harvester (rectangular beam), and the

Table 2 Performance comparison table of optimal structure data and single item optimal structure data comparison table

Structure	Optimal beam length structure	Optimal beam width structure	Optimal PZT structure	Comprehensive optimal structure
Voltage (V)	0.1220	0.1814	0.1705	0.2433
Voltage increase ratio (based on the optimum beam length structure)	0.00%	48.69%	39.75%	99.43%
Power (W)	5.610e−7	6.711e−7	6.999e−7	7.701e−7
Power increase ratio (based on the optimum beam length structure)	0.00%	19.63%	24.76%	37.27%

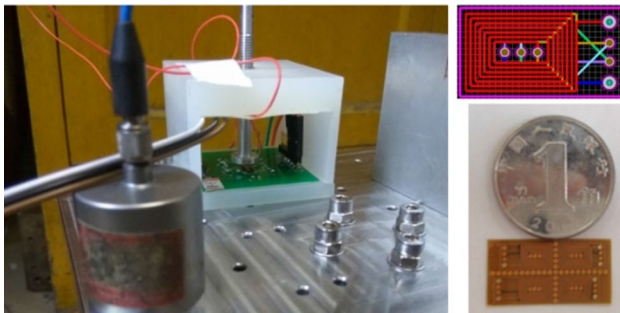


Fig. 23 MEMS coupled piezoelectric–electromagnetic energy harvester prototype test

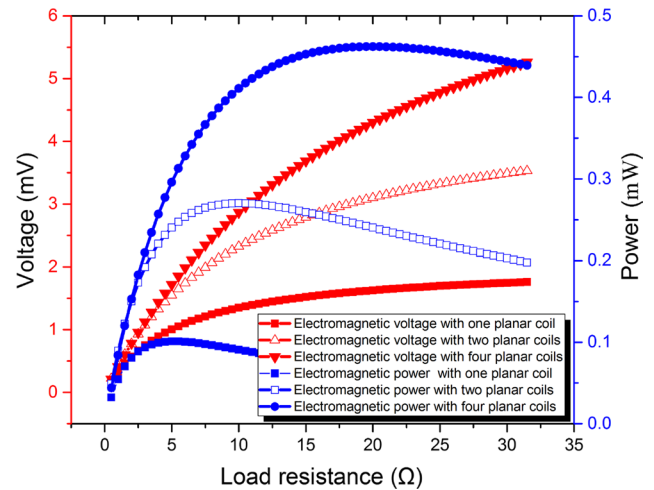


Fig. 25 Electromagnetic loading characteristics of MEMS coupled energy harvester

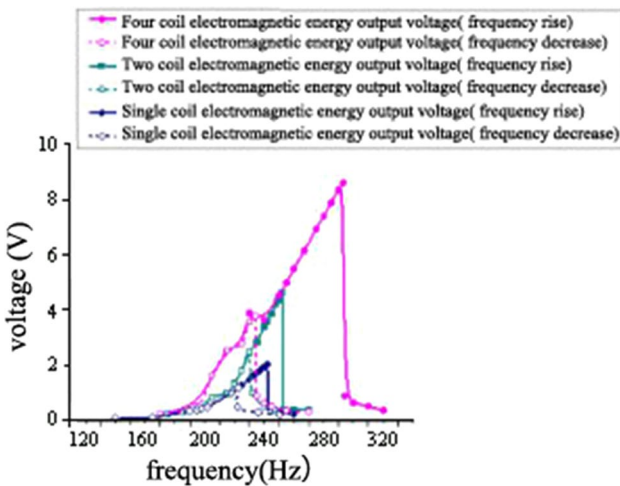


Fig. 24 The opening circuit voltage of MEMS coupled piezoelectric–electromagnetic energy harvester

Table 3 Designed parameters of coupled piezoelectric-electromagnetic energy harvester

Type	Number of coils	Piezoelectric chip number	Distance between coils and permanent magnets (mm)
Coupled 1	6 layer × 1	1	1
Coupled 2	6 layer × 2	1	1
Coupled 3	6 layer × 4	1	1
Coupled 4	6 layer × 4	2	1

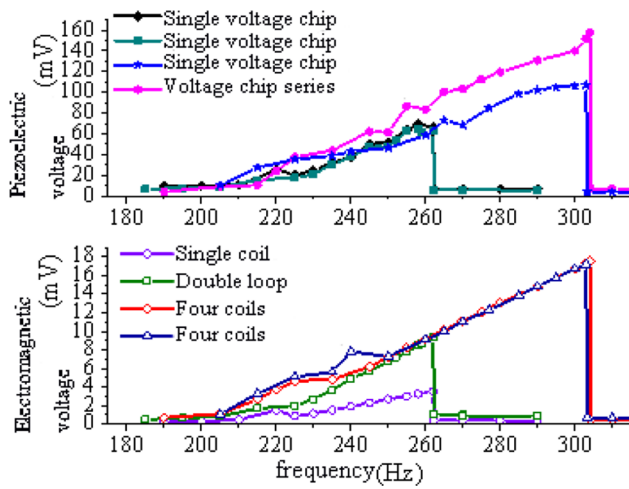


Fig. 26 Electromagnetic opening circuit voltage of coupled MEMS energy harvester

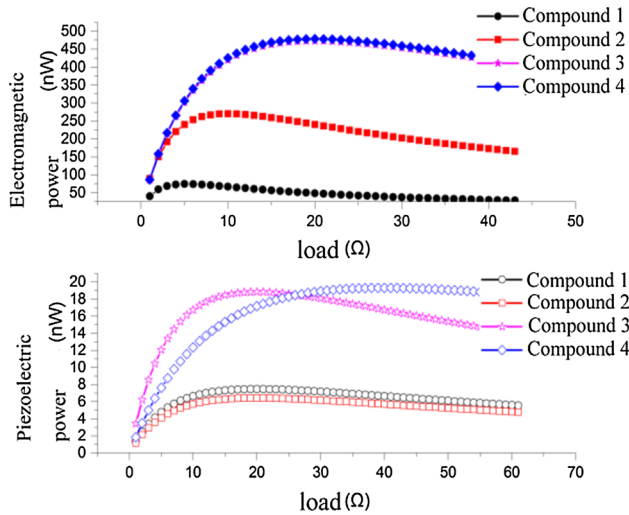


Fig. 27 Electromagnetic load characteristics of coupled MEMS energy harvester

piezoelectric output voltage is increased 18.89%; the electromagnetic output voltage of the 6th coupled energy harvester is slightly lower than the 5th; from the comprehensive analysis the total power output of the 6th coupled energy harvester is 2.26% higher than the 5th.

6 Summary

This paper studies the optimization design, processing technology and structural performance test of the coupled MEMS piezoelectric–electromagnetic energy harvester. The piezoelectric structure is optimized designed by ANSYS software. The MEMS process design and implementation of the optimized structure is carried out, and the comparative analysis of the prototype is done. The analysis results show that after introducing the large deformation nonlinearity, the energy harvesting band of MEMS structure has been greatly broadened, and the use of planar multilayer microcoils makes the characteristics of electromagnetic capture energy more significant. In addition, the analysis also shows that compared with the single piezoelectric energy harvesting mode, the nonlinear effect of the coupled energy harvester is enhanced, the capture frequency band is broadened, and the output performance is improved significantly. MEMS coupled

Table 4 Output performance of coupled piezoelectric-electromagnetic energy harvester

Type	Piezoelectricity		Electromagnetism		Composite power (nW)	Performance	Bandwidth (Hz)
	Voltage (mV)	Power (nW)	Voltage (mV)	Power (nW)			
Single piezoelectricity	81.98	10.50×4	–	–	42.00	–	10
Coupled 1	69.18	7.61×4	3.52	74.43	104.87	↑1.50 times	15
Coupled 2	64.14	6.43×4	9.30	270.28	296.00	↑6.05 times	17
Coupled 3	109.81	18.84×4	17.21	473.06	548.42	↑12.06 times	38
Coupled 4	157.26	19.32×4	17.52	478.52	555.80	↑12.23 times	41

↑ represents performance improvement

Table 5 Comparison of structural parameters between coupled piezoelectric and electromagnetic rectangular beams and trapezoid beams

Type	Structure	Coil	Coil and detection quality	Test quality size (mm)	Piezoelectric connection
Coupled 5	Rectangular beam	6 layer×4	0.1	3.5×3.5×0.8	Single beam series
Coupled 6	Trapezoidal beam	6 layer×4	0.1	3.5×3.5×0.8	Single beam series

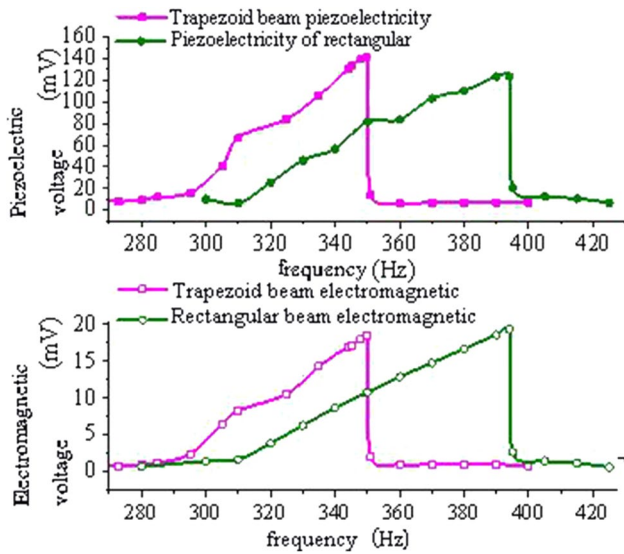


Fig. 28 Comparison of opening circuit voltage of piezoelectricity and electromagnetic

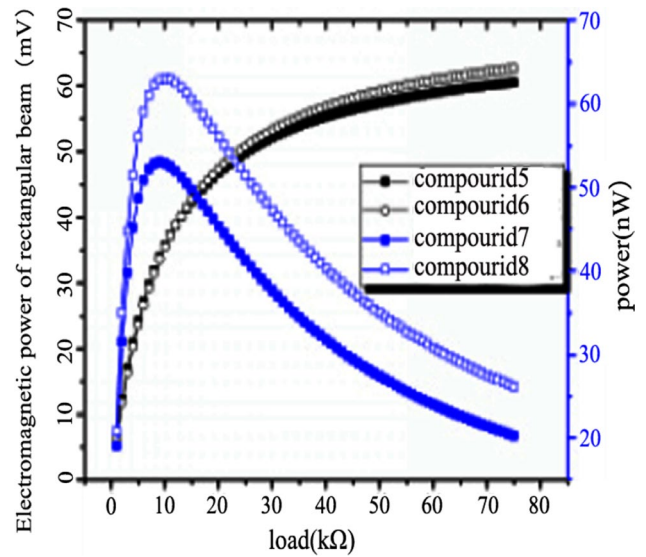


Fig. 30 Piezoelectric loading characteristics

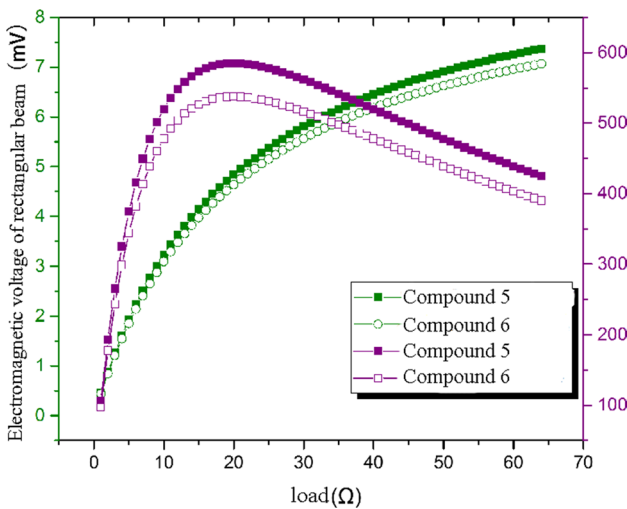


Fig. 29 Electromagnetic loading characteristics

piezoelectric–electromagnetic energy harvester with the electromagnetic coil and four piezoelectric in series is increased 12.23 times in power; in addition, the output voltage and couple power of the coupled energy harvester with piezoelectric beam structure is increased 18.89% times and 2.26% times.

Table 6 Comparison of the output performance of coupled piezoelectric and electromagnetic rectangular beams and trapezoid beams

Type	Piezoelectricity		Electromagnetism		Composite power (nW)	Piezoelectric/composite performance
	Voltage (mV)	Power (nW)	Voltage (mV)	Power (nW)		
Coupled 5	123.55	53.00×4	19.35	570.04	782.04	–
Coupled 6	142	63.01×4	18.55	547.66	799.70	↑18.89%/↑2.26%

↑ represents performance of Piezoelectric and composite improvement compared to the Coupled 5

Acknowledgements This work supported by the Natural Science Foundation of Shandong Province, China (ZR201709220253).

References

- Inman, D. J., & Karami, M. A. (2012). Powering pacemakers from heartbeat vibrations using linear and nonlinear energy harvesters. *Applied Physics Letters*, 100(4), 042901–042904.
- Ling, C. S., Hewitt, D., Burrow, S. G., Clare, L., Barton, D. A. W., Wells, D. M., et al. (2013). Technological challenges of developing wireless health and usage monitoring systems. *Proceedings of SPIE*, 8695(1), 86950.
- Nicholas, R., & Natarajan, B. (2013). A structured approach to optimization of energy harvesting. In *Wireless sensor networks the 10th annual IEEE CCNC* (pp. 420–425).
- Tiwari, R., Buch, N., & Garcia, E. (2014). Energy balance for peak detection method in piezoelectric energy harvester. *Journal of Intelligent Material Systems and Structures*, 25(8), 1024–1035.
- Wacharasindhu, T., & Wkwon, J. (2008). A micromachined energy harvester from a keyboard using combined electromagnetic and piezoelectric conversion. *Journal of Micromechanics and Microengineering*, 18(10), 1–8.
- Yang, X., Wang, Y., & Cao, Y. (2014). A new hybrid piezoelectric–electromagnetic vibration-powered generator and its model and experiment research applied superconductivity. *IEEE Transactions on Applied Superconductivity*, 24(3), 1–4.
- Challa, V. R., Prasad, M. G., & Fisher, F. T. (2009). A coupled piezoelectric–electromagnetic energy harvesting technique for achieving increased power output through damping matching. *Smart Materials and Structures*, 18(9), 1–11.
- Robert, D., Wu, W. J., & Chen, Y. Y. (2008). A hybrid piezoelectric and electromagnetic energy harvesting device. In *19th International conference on AST*.
- Tadesse, Y., Zhang, S., & Priya, S. (2009). Multimodal energy harvesting system: Piezoelectric and electromagnetic. *Journal of Intelligent Material Systems and Structures*, 20(5), 625–632.
- Li, P., Gao, S., & Cai, H. (2014). Coupling effect analysis for hybrid piezoelectric and electromagnetic energy harvesting from random vibrations. *International Journal of Precision Engineering and Manufacturing*, 9(15), 1915–1924.
- Li, P., Gao, S., & Niu, S. (2014). An analysis of the coupling effect for a hybrid piezoelectric and electromagnetic energy harvester. *Smart Materials and Structures*, 23(6), 065016.
- Li, P., Gao, S., & Cai, H. (2016). Theoretical analysis and experimental study for nonlinear hybrid piezoelectric and electromagnetic energy harvester. *Microsystem Technologies*, 22(4), 727–739.
- Li, P., Gao, S., & Zhou, X. (2018). On the performances of a nonlinear hybrid piezoelectric and electromagnetic energy harvester. *Microsystem Technologies*, 24(2), 1017–1024.
- Marin, A., Turner, J., & Ha, D. S. (2013). Broadband electromagnetic vibration energy harvesting system for powering wireless sensor nodes. *Smart Materials and Structures*, 22(7), 075008.
- Khan, S. F. U. (2011). *Vibration-based electromagnetic energy harvesters for MEMS application*. Vancouver, CA: The University of British Columbia.
- Yang, B., Lee, C., & Kee, W. L. (2010). Hybrid energy harvester based on piezoelectric and electromagnetic mechanisms. *Journal of Micro/Nanolithography, MEMS, and MOEMS*, 9(2), 1–10.

Publisher's Note Springer Nature remains neutral with regard to jurisdictional claims in published maps and institutional affiliations.



Lian-min Cao (1978), Lingxian city of Shandong province's people, associate professor, master supervisor, PhD, main research interests include mechanical and electrical hydraulic control, mining machinery and so on. And published more than 50 papers at home and abroad journals, of which 2 were SCI search and 21 were EI search included.



Zhi-xu Li (1995), Jining city of Shandong province's people, assistant engineer, graduate student of Shandong University of Science and Technology. The main research direction is electro hydraulic control and automation and published a Chinese core journals and two utility model patents.



Cheng Guo (1993), Taian city of Shandong province's people, assistant engineer, graduate student of Shandong University of Science and Technology. The main research direction is electro hydraulic control and automation and published a Chinese core journals and two utility model patents.



Ting-ming Wang (1995), Jinan city of Shandong province's people, assistant engineer, graduate student of Shandong University of Science and Technology. The main research direction is electro hydraulic control and automation and published a Chinese core journals and two utility model patents.



Peng-peng Li (1993), Heze city of Shandong province's people, assistant engineer, graduate student of Shandong University of Science and Technology. The major is mechanical engineering. The research direction is the system on coal mine comprehensive Information, and published three utility model patents.



Xiang-qiang Meng (1994), Rizhao city of Shandong province's people, assistant engineer, graduate student of Shandong University of Science and Technology. The main research direction is electro hydraulic control and automation and published a Chinese core journals and two utility model patents.